PASSIVITY-BASED PARAMETER ESTIMATION AND COMPOSITE ADAPTIVE POSITION CONTROL OF INDUCTION MOTORS

Jenn-Yih Chen
Department of Mechanical and Computer-Aided Engineering, National Formosa University, Yunlin County, Taiwan
E-mail: jychen@nfu.edu.tw

ICETI 2012-I1037_SCI
No. 13-CSME-42, E.I.C. Accession 3500

ABSTRACT

In the rotor reference frame, the input-output linearization theory was adopted to decouple the rotor position and rotor flux. We then designed two adaptation laws to estimate the rotor resistance and mechanical parameters of the motor. The passive properties of the negative feedback connection from the rotor flux observer to the rotor resistance estimator, and the position controller were analyzed according to the passivity theorem. The overall control system was proved to be globally stable. Finally, experimental results show that the proposed scheme is robust to the variations of the rotor resistance and load torque disturbances. Furthermore, the estimated parameters can converge to the actual values.

Keywords: rotor resistance; composite adaptive control; passivity theorem; globally stable.

PARAMÈTRES D'ESTIMATION AXÉS SUR LA PASSIVITÉ ET LA COMMANDE ADAPTIVE COMPOSITE DE MOTEURS À INDUCTION

RÉSUMÉ

Dans le cadre de référence du rotor, la théorie de linéarisation entrée-sortie a été adoptée pour dissocier la position du rotor et le flux du rotor. Nous avons alors conçu deux lois adaptives pour estimer la résistance du rotor et les paramètres mécaniques du rotor. Les propriétés passives de la rétroaction négative de la connection, à partir de l'observateur de flux du rotor, et le contrôleur de position furent analysées selon le théorème de la passivité. Le système général de commande démontre qu'il est globalement stable. Finalement, les résultats des expériences ont démontrés que le schème proposé est robuste pour de qui concerne les variations de la résistance du rotor et les perturbations du couple de charge. De plus, les paramètres estimés peuvent converger avec les valeurs courantes.

Mots-clés : résistance du rotor ; commande adaptive composite ; théorème de la passivité ; globalement stable.

1. INTRODUCTION

Owing to rapid improvements in microprocessors and power electronic devices, the vector field orientation approach [1] has made induction motors widely used in high-performance applications [2]. The dynamic behavior of induction motors is rather similar to that of separately excited dc motors by adopting the field-oriented or feedback linearization techniques, and therefore the control efforts can be reduced. Unfortunately, the rotor resistance may vary due to the change of operating temperature and the saturation of the magnetizing inductance. The variations of the rotor resistance or unknown external disturbances will affect accuracy of stator current components and output responses.

With generalized energy considerations, the passivity theorem is a system theoretic concept that provides a basic framework for the stability analysis of nonlinear dynamic systems [3]. Espinosa and Ortega [4] presented a passivity-based method for the control of an induction motor without the explicit implementation of a rotor flux observer. A passivity-based approach was developed to force induction motors to track time-varying speed and position without employing any knowledge of rotor's electrical state variables [5]. Peresada et al. [6] proposed two new indirect field-oriented speed-flux tracking controllers, and the design of the control algorithms was based on the passivity theorem. For controlling the speed of a permanent magnet synchronous motor, Petrovic et al. [7] developed the energy-shaping strategy to design an almost globally convergent controller. Recently, some passivity-based schemes were presented for induction motors or permanent magnet synchronous motors control, and the effectiveness was demonstrated by numerical simulations [8, 9]. A passivity-based speed controller was proposed for a sensorless synchronous reluctance motor [10]. The presented drive system had good position tracking responses and it was robust to load torque disturbances. Two design techniques were proposed to control and reduce the vibration of a linear switched reluctance motor, and the analyzed structures were compared by adopting the simulation and experimental results [11].

Although the stability of the passivity-based controller is global, parametric uncertainties of induction motors still affect the control performance. The main uncertainties are caused by thermal variations and load torques. Generally speaking, the adaptive control is an efficient method to deal with these problems. In this paper, a composite adaptive controller uses both system output and control input to design the adaptation law. The position control system is formally proved by the passivity theorem, and the design methodology for the proposed controller is also presented. In addition, the estimated parameters are all bounded, and the asymptotically stable property of the system can be proved when the reference position command is a sinusoidal signal with two different frequencies. Experimental results are provided to demonstrate the effectiveness of the proposed scheme.

2. MATHEMATICAL MODEL OF THE CURRENT-FED INDUCTION MOTOR

The dynamics of an induction motor is more complicated in the three-phase ($a-b-c$) system. Thus, an equivalent two-phase model (d–q) is often employed to simplify the complexity of the differential equations. The stator variables of d–q axes in the arbitrary reference frame can be obtained from the three-phase variables, and can be expressed as [2]

$$\begin{bmatrix} f_{ds} \\ f_{qs} \end{bmatrix} = \frac{2}{3} \begin{bmatrix} \sin\theta & \sin(\theta - 2\pi/3) & \sin(\theta + 2\pi/3) \\ \cos\theta & \cos(\theta - 2\pi/3) & \cos(\theta + 2\pi/3) \end{bmatrix} \begin{bmatrix} f_{as} \\ f_{bs} \\ f_{cs} \end{bmatrix}, \tag{1}$$

where f represents the current, voltage, or flux linkage; $\theta = 0$ (q^s-axis is aligned with the as-axis) for the stationary, $\theta = \theta_r$ (rotor angle) for the rotor, and $\theta = \theta_e$ (angle of synchronously rotating frame) for the synchronously rotating reference frame. Hereinafter, we use the superscripts s, r, and e to denote these three different reference frames, respectively. The corresponding inverse matrix of Eq. (1) is

$$\begin{bmatrix} f_{as} \\ f_{bs} \\ f_{cs} \end{bmatrix} = \begin{bmatrix} \sin\theta & \cos\theta \\ \sin(\theta - 2\pi/3) & \cos(\theta - 2\pi/3) \\ \sin(\theta + 2\pi/3) & \cos(\theta + 2\pi/3) \end{bmatrix} \begin{bmatrix} f_{ds} \\ f_{qs} \end{bmatrix}. \tag{2}$$

The stator variables on the d^s–q^s axes can be converted into the d^r–q^r frame as

$$\begin{bmatrix} f_{ds}^r \\ f_{qs}^r \end{bmatrix} = \begin{bmatrix} \cos(n_p\theta_m) & \sin(n_p\theta_m) \\ -\sin(n_p\theta_m) & \cos(n_p\theta_m) \end{bmatrix} \begin{bmatrix} f_{ds}^s \\ f_{qs}^s \end{bmatrix}, \tag{3}$$

where n_p and $\theta_m (= \theta_r/n_p)$ represent the number of pole pairs and mechanical rotor position, respectively.

Assuming an induction motor is driven by a current-regulated voltage source inverter, the dynamics of the motor in the $d^r - q^r$ frame can be described by the following differential equations:

$$\dot{\boldsymbol{\lambda}}_r^r + \frac{R_r}{L_r}\boldsymbol{\lambda}_r^r = \frac{MR_r}{L_r}\mathbf{i}_s^r, \tag{4}$$

$$\ddot{\theta}_m + \frac{B}{J}\dot{\theta}_m = \frac{k_t}{J}\boldsymbol{\lambda}_r^{rT}\mathbf{E}\mathbf{i}_s^r - \frac{1}{J}T_L, \tag{5}$$

where

$$k_t = \frac{3Mn_p}{2L_r} \quad \text{and} \quad \mathbf{E} = \begin{bmatrix} 0 & 1 \\ -1 & 0 \end{bmatrix}.$$

$\boldsymbol{\lambda}_r^r = [\lambda_{dr}^r \quad \lambda_{qr}^r]^T$ and $\mathbf{i}_s^r = [i_{ds}^r \quad i_{qs}^r]^T$ denote the d^r–q^r axes rotor flux linkages and stator currents, respectively. R_r, L_r, and M are the rotor resistance, rotor inductance, and magnetizing inductance, respectively. J, B, and T_L denote the moment of inertia of motor and load, viscous friction coefficient, and load torque, respectively. The superscript "T" represents the matrix transposition.

Employing the input-output linearization method, the rotor flux amplitude is defined as

$$\varphi = \sqrt{\boldsymbol{\lambda}_r^{rT}\boldsymbol{\lambda}_r^r}. \tag{6}$$

Differentiate Eq. (6) and use Eq. (4) to yield

$$\dot{\varphi} + \frac{R_r}{L_r}\varphi = \frac{MR_r}{L_r\varphi}\boldsymbol{\lambda}_r^{rT}\mathbf{i}_s^r. \tag{7}$$

Two new control inputs u_1 and u_2 are defined as

$$\begin{bmatrix} u_1 \\ u_2 \end{bmatrix} = \begin{bmatrix} \lambda_{dr}^r/\varphi & \lambda_{qr}^r/\varphi \\ -\lambda_{qr}^r & \lambda_{dr}^r \end{bmatrix} \mathbf{i}_s^r = \begin{bmatrix} \cos\theta_{sl} & \sin\theta_{sl} \\ -\varphi\sin\theta_{sl} & \varphi\cos\theta_{sl} \end{bmatrix} \mathbf{i}_s^r, \tag{8}$$

where θ_{sl} is the angle between φ and d^r-axis. From the geometric relation of different reference frames [2], we obtain $u_1 = i_{ds}^e$ and $u_2 = \varphi i_{qs}^e$. Thus, Eqs. (5) and (7) can be rewritten as

$$\ddot{\theta}_m + \frac{B}{J}\dot{\theta}_m = \frac{k_t}{J}u_2 - \frac{1}{J}T_L, \tag{9}$$

$$\dot{\varphi} + \frac{R_r}{L_r}\varphi = \frac{MR_r}{L_r}u_1. \tag{10}$$

Equations (9) and (10) show the mechanical rotor position and rotor flux dynamics are fully decoupled. The control inputs u_2 and u_1 can be adopted to control the rotor position and rotor flux amplitude, respectively.

3. DESIGN OF THE ROTOR RESISTANCE ESTIMATOR

This paper is aimed at positioning control of induction motors. An open-loop current model rotor flux observer is suitable for flux estimation owing to it is effective at lower speed ranges, and can be given as

$$\dot{\hat{\boldsymbol{\lambda}}}_r^r + \frac{\hat{R}_r}{L_r}\hat{\boldsymbol{\lambda}}_r^r = \frac{M\hat{R}_r}{L_r}\mathbf{i}_s^r, \tag{11}$$

where the superscript "ˆ" denotes the estimated value.

Subtracting Eq. (4) from Eq. (11), and adding the term $R_r\hat{\boldsymbol{\lambda}}_r^r/L_r$ on both sides to get

$$\dot{\tilde{\boldsymbol{\lambda}}}_r^r + \frac{R_r}{L_r}\tilde{\boldsymbol{\lambda}}_r^r = \frac{\tilde{R}_r}{L_r}(M\,\mathbf{i}_s^r - \hat{\boldsymbol{\lambda}}_r^r), \tag{12}$$

where

$$\tilde{\boldsymbol{\lambda}}_r^r = \hat{\boldsymbol{\lambda}}_r^r - \boldsymbol{\lambda}_r^r, \quad \tilde{R}_r = \hat{R}_r - R_r. \tag{13}$$

The rotor resistance estimator was designed to possess passive property, and it was chosen as

$$\dot{\hat{R}}_r = -g_1\,(M\,\mathbf{i}_s^r - \hat{\boldsymbol{\lambda}}_r^r)^T\tilde{\boldsymbol{\lambda}}_r^r, \quad g_1 > 0, \tag{14}$$

where g_1 is the adaptation gain. Figure 1 shows the negative feedback connection from the rotor flux observer to the rotor resistance estimator. In order to use the passivity theorem to prove the stability of the observer and the estimator, we have to analyze passive properties of each block in Fig. 1. Using Eq. (12) then gives

$$\begin{aligned}\left\langle \tilde{\boldsymbol{\lambda}}_r^r,\ \frac{\tilde{R}_r(M\mathbf{i}_s^r - \hat{\boldsymbol{\lambda}}_r^r)}{L_r}\right\rangle_t &= \frac{1}{L_r}\int_0^t \tilde{\boldsymbol{\lambda}}_r^{rT}\,\tilde{R}_r(M\,\mathbf{i}_s^r - \hat{\boldsymbol{\lambda}}_r^r)\,d\tau \\ &= \frac{1}{2}\left(\tilde{\boldsymbol{\lambda}}_r^{rT}(t)\tilde{\boldsymbol{\lambda}}_r^r(t) - \tilde{\boldsymbol{\lambda}}_r^{rT}(0)\tilde{\lambda}_r^r(0)\right) \\ &\quad + \frac{R_r}{L_r}\int_0^t \tilde{\boldsymbol{\lambda}}_r^{rT}\tilde{\boldsymbol{\lambda}}_r^r\,d\tau, \quad \forall t \geq 0,\end{aligned} \tag{15}$$

where $\langle\ ,\ \rangle_t$ is the inner product operator. Following Eq. (15), the mapping $\tilde{R}_r(M\,\mathbf{i}_s^r - \hat{\boldsymbol{\lambda}}_r^r)/L_r \mapsto \tilde{\boldsymbol{\lambda}}_r^r$ of the feedforward block is an output strictly passive system [12]. Employing Eqs. (13) and (14) to obtain

$$\begin{aligned}\left\langle -\frac{\tilde{R}_r(M\,\mathbf{i}_s^r - \hat{\boldsymbol{\lambda}}_r^r)}{L_r}, \tilde{\boldsymbol{\lambda}}_r^r\right\rangle_t &= -\frac{1}{L_r}\int_0^t \tilde{R}_r(M\,\mathbf{i}_s^r - \hat{\boldsymbol{\lambda}}_r^r)^T\tilde{\boldsymbol{\lambda}}_r^r d\tau \\ &= \frac{1}{2g_1L_r}\left(\tilde{R}_r^2(t) - \tilde{R}_r^2(0)\right), \quad \forall t \geq 0\end{aligned} \tag{16}$$

The mapping $\tilde{\boldsymbol{\lambda}}_r^r \mapsto -\tilde{R}_r(M\,\mathbf{i}_s^r - \hat{\boldsymbol{\lambda}}_r^r)/L_r$ of the feedback block is a lossless system [12]. Adding Eqs. (15) and (16) yields

$$\tilde{\boldsymbol{\lambda}}_r^{rT}(t)\tilde{\boldsymbol{\lambda}}_r^r(t) + \frac{\tilde{R}_r^2(t)}{g_1L_r} \leq \tilde{\boldsymbol{\lambda}}_r^{rT}(0)\tilde{\boldsymbol{\lambda}}_r^r(0) + \frac{\tilde{R}_r^2(0)}{g_1L_r}. \tag{17}$$

Therefore, we have $\tilde{\lambda}_r^r$ and $\tilde{R}_r \in L_\infty$. $\mathbf{i}_s^r$ and R_r are bounded, it can be shown that $\hat{\boldsymbol{\lambda}}_r^r$ and $\hat{R}_r \in L_\infty$ in Eqs. (11) and (13). This means that $\dot{\tilde{\boldsymbol{\lambda}}}_r^r \in L_\infty$ in Eq. (12). Furthermore, Eq. (17) gives

$$\int_0^t \tilde{\boldsymbol{\lambda}}_r^{rT}\tilde{\boldsymbol{\lambda}}_r^r\,d\tau \leq \frac{L_r}{2R_r}\left(\tilde{\boldsymbol{\lambda}}_r^{rT}(0)\tilde{\boldsymbol{\lambda}}_r^r(0) + \frac{\tilde{R}_r^2(0)}{g_1L_r}\right). \tag{18}$$

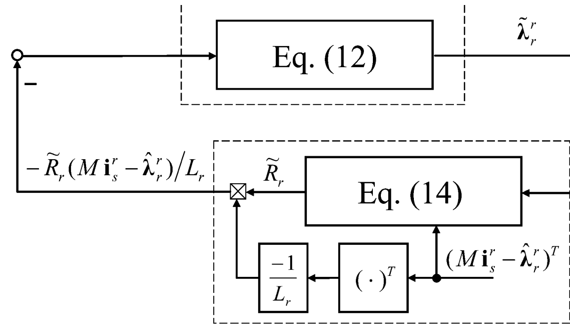

Fig. 1. Feedback connection of the rotor flux observer to the rotor resistance estimator.

Equation (18) implies that $\tilde{\boldsymbol{\lambda}}_r^r \in L_2$, and $\tilde{\boldsymbol{\lambda}}_r^r \to 0$ as $t \to \infty$ by Barbalat's lemma [13]. And further, $\ddot{\tilde{\boldsymbol{\lambda}}}_r^r \in L_\infty$, $\tilde{\boldsymbol{\lambda}}_r^r \to 0$, and $\dot{\tilde{\boldsymbol{\lambda}}}_r^r \to 0$ as $t \to \infty$, which implies that Eq. (12) satisfies the following condition:

$$\tilde{R}_r(M\mathbf{i}_s^r - \hat{\boldsymbol{\lambda}}_r^r)/L_r = 0 \text{ as } t \to \infty. \tag{19}$$

Suppose the term $(M\mathbf{i}_s^r - \hat{\boldsymbol{\lambda}}_r^r)/L_r$ in Eq. (19) satisfies the inequality

$$\int_t^{t+\varepsilon} \left(\frac{M\mathbf{i}_s^r - \hat{\boldsymbol{\lambda}}_r^r}{L_r}\right)\left(\frac{M\mathbf{i}_s^r - \hat{\boldsymbol{\lambda}}_r^r}{L_r}\right)^T d\tau \geq \eta\mathbf{I} > 0, \quad \forall t \geq 0, \tag{20}$$

where ε and η are positive constants, and $\mathbf{I}$ is an identity matrix. Equations (12) and (14) satisfy the persistent excitation condition [13] and $\tilde{R}_r \to 0$. Hence, the above proves that the negative feedback connection of Fig. 1 is asymptotically stable.

4. DESIGN OF THE COMPOSITE ADAPTIVE POSITION CONTROLLER

In a conventional model reference adaptive control, only the output tracking error is utilized for designing adaptation laws and the performance is limited by adaptation gains and reference input commands. It is known that small adaptation gains lead the estimated parameters to slow convergence to the actual values and more transient tracking errors. Conversely, large adaptation gains speed up adaptation which implies a faster convergence of parameters. When the control input is not perfect, such as in a saturation situation, excessive adaptation will happen. This will lead to slow convergence of the parameters and large transient tracking errors. The principle of a composite adaptation law combines the tracking error based adaptation law and the prediction error based estimation law [14]. That is, a composite adaptive controller uses both system output and control input to design the parameter estimation law, and speed up the convergent rate of the tracking errors and controller parameters of the system.

Generally, induction motors are used as speed (or positioning) actuators to drive various mechanical loads. These typical load torques can be described by the torque-speed characteristic curve, therefore a sinusoidal load torque which is a function of the mechanical rotor position can be described as

$$T_L = K_L \sin(\theta_m), \tag{21}$$

where K_L is an unknown constant. Substitute Eq. (21) into Eq. (9) to get

$$[\ \ddot{\theta}_m \quad \dot{\theta}_m \quad \sin(\theta_m)\ ]\mathbf{Q} = u_2, \tag{22}$$

where $\mathbf{Q} = [J/k_t \quad B/k_t \quad K_L/k_t]^T = [J_k \quad B_k \quad K_k]^T$. Choose the control input

$$u_2 = \mathbf{\Phi}^T \hat{\mathbf{Q}} - g_2 S, \quad g_2 > 0, \tag{23}$$

where

$$\begin{aligned} \mathbf{\Phi} &= [\ddot{\theta}_m^* - g_3 \dot{e}_\theta \quad \dot{\theta}_m^* - g_3 e_\theta \quad \sin(\theta_m)]^T, \quad e_\theta = \theta_m - \theta_m^*, \\ \hat{\mathbf{Q}} &= [\hat{J}_k \quad \hat{B}_k \quad \hat{K}_k]^T, \quad S = \dot{e}_\theta + g_3 > 0, \end{aligned} \tag{24}$$

where e_θ, $\hat{\mathbf{Q}}$, and the superscript "*" are the position tracking error, *a priori* estimates of $\mathbf{Q}$, and the command or the reference input, respectively. Substituting Eq. (23) into Eq. (22) yields

$$J_k \dot{S} + (B_k + g_2) S = \mathbf{\Phi}^T \tilde{\mathbf{Q}}, \tag{25}$$

where $\tilde{\mathbf{Q}}$ denotes the parameter estimation error that is defined as

$$\tilde{\mathbf{Q}} = \hat{\mathbf{Q}} - \mathbf{Q} = [\hat{J}_k - J_k \quad \hat{B}_k - B_k \quad \hat{K}_k - K_k]^T \tag{26}$$

In order to estimate the parameter $\mathbf{Q}$, the composite adaptation law was designed as

$$\dot{\tilde{\mathbf{Q}}}(t) = -\mathbf{\Gamma}^{-1} \mathbf{\Phi} S - \delta \mathbf{\Lambda} \int_0^t e^{-\delta(1-t)} \mathbf{W}(\tau) \mathbf{W}^T(\tau) \tilde{\mathbf{Q}}(t) d\tau \tag{27}$$

where $\mathbf{\Gamma}^{-1}$ and $\mathbf{\Lambda}$ are both the adaptation gains and diagonal positive definite matrices. δ represents the forgetting factor which can reduce the influence of past feedback signals. $\mathbf{W}$ denotes a signal vector which is relevant to the system output, and it is defined as

$$\mathbf{W} = \frac{\kappa}{p + \kappa} [\ddot{\theta}_m \quad \dot{\theta}_m \quad \sin(\theta_m)]^T, \tag{28}$$

where κ is a positive constant, and p is the differential operator (d/dt). Using (26), Eq. (27) can be rewritten as

$$\dot{\tilde{\mathbf{Q}}}(t) = \dot{\hat{\mathbf{Q}}}(t) = -\mathbf{\Gamma}^{-1} \mathbf{\Phi} S - \mathbf{\Lambda} \mathbf{F}(t) \tilde{\mathbf{Q}}(t) = -\mathbf{\Gamma}^{-1} \mathbf{\Phi} S - \mathbf{\Lambda} \mathbf{F}(t) \hat{\mathbf{Q}}(t) + \mathbf{\Lambda} \mathbf{G}(t), \tag{29}$$

where

$$\begin{aligned} \mathbf{F}(t) &= \delta \int_0^t e^{-\delta(t-\tau)} \mathbf{W}(\tau) \mathbf{W}^T(\tau) d\tau, \\ \mathbf{G}(t) &= \delta \int_0^t e^{-\delta(t-\tau)} \mathbf{W}(\tau) u_f(\tau) d\tau, \quad u_f = \frac{\kappa}{p + \kappa} u_2. \end{aligned} \tag{30}$$

It is noted that the time derivative of Eq. (30) is utilized for implementing the composite adaptive position controller, i.e.,

$$\begin{aligned} \dot{\mathbf{F}}(t) &= -\delta \mathbf{F}(t) + \delta \mathbf{W}(t) \mathbf{W}^T(t), \quad \mathbf{F}(0) = 0, \\ \dot{\mathbf{G}}(t) &= -\delta \mathbf{G}(t) + \delta \mathbf{W}(t) u_f(t), \quad \mathbf{G}(0) = 0. \end{aligned} \tag{31}$$

Thus, Fig. 2 shows the equivalent closed loop dynamic system for the position controller of an induction motor.

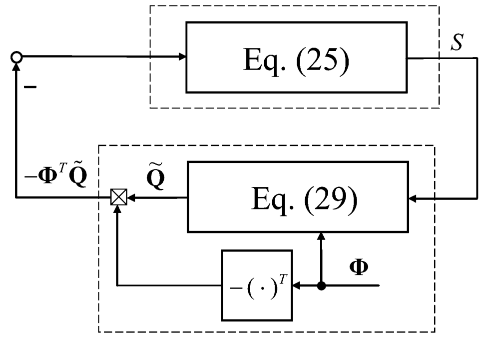

Fig. 2. Equivalent closed loop system for position controller.

From Eq. (25), we have

$$\left\langle S,\ \mathbf{\Phi}^T\tilde{\mathbf{Q}}\right\rangle_t = \frac{1}{2}(J_kS^2(t) - J_kS^2(0)) + (B_k + g_2)\int_0^t S^2 d\tau, \forall t \geq 0 \tag{32}$$

Hence, the mapping $\mathbf{\Phi}^T\tilde{\mathbf{Q}} \mapsto S$ of the feedforward block in Fig. 2 is an output strictly passive system. Employing Eq. (29) we obtain

$$\left\langle -\mathbf{\Phi}^T\tilde{\mathbf{Q}}, S\right\rangle_t = \frac{1}{2}(\tilde{\mathbf{Q}}^T(t)\mathbf{\Gamma}\tilde{\mathbf{Q}}(t) - \tilde{\mathbf{Q}}^T(0)\mathbf{\Gamma}\tilde{\mathbf{Q}}(0)) + \int_0^t \tilde{\mathbf{Q}}^T\mathbf{\Gamma}\mathbf{\Lambda}\mathbf{F}\tilde{\mathbf{Q}}d\tau, \quad \forall t \geq 0. \tag{33}$$

From Eq. (33), if $\mathbf{F}(t)$ is a positive definite matrix, $\mathbf{W}(t)$ is persistently exciting, which implies that the mapping $S \mapsto -\mathbf{\Phi}^T\tilde{\mathbf{Q}}$ of the feedback block is an output strictly passive system. Adding Eqs. (32) and (33) gives

$$J_kS^2(t) + \tilde{\mathbf{Q}}^T(t)\mathbf{\Gamma}\tilde{\mathbf{Q}}(t) < J_kS^2(0) + \tilde{\mathbf{Q}}^T(0)\mathbf{\Gamma}\tilde{\mathbf{Q}}(0). \tag{34}$$

Equation (34) implies that the filtered tracking error S and the parameter estimation error $\tilde{\mathbf{Q}}$ will converge to zero asymptotically. Therefore, the proposed composite adaptive position control system for an induction motor drive is asymptotically stable. If $\mathbf{F}(t)$ is not a positive definite matrix, $\mathbf{W}(t)$ is not persistently exciting, which implies that the mapping $S \mapsto -\mathbf{\Phi}^T\tilde{\mathbf{Q}}$ of the feedback block is a lossless system. Combining Eqs. (32) and (33), we obtain

$$J_kS^2(t) + \tilde{\mathbf{Q}}^T(t)\mathbf{\Gamma}\tilde{\mathbf{Q}}(t) \leq J_kS^2(0) + \tilde{\mathbf{Q}}^T(0)\mathbf{\Gamma}\tilde{\mathbf{Q}}(0). \tag{35}$$

Thus, Eq. (35) implies that S, $\tilde{\mathbf{Q}}$, $\mathbf{\Phi}^T\tilde{\mathbf{Q}} \in L_\infty$, and $\dot{S} \in L_\infty$ according to Eq. (25). That is, $\dot{e}_\theta \in L_\infty$, $\ddot{e}_\theta \in L_\infty$, and $\dot{e}_\theta$ is uniformly continuous based on the theorem [15]. Furthermore, using Eqs. (32) and (33) yields

$$\int_0^t S^2 d\tau \leq \frac{1}{2(B_k + g_2)}(J_kS^2(0) + \tilde{\mathbf{Q}}^T(0)\mathbf{\Gamma}\tilde{\mathbf{Q}}(0)). \tag{36}$$

Equation (36) means that $S \in L_2$, and it follows from the theorem [15] that $e_\theta \in L_2 \cap L_\infty$, $\dot{e}_\theta \in L_2$, e_θ is continuous, and $e_\theta \to 0$ as $t \to \infty$. The above proves that $\dot{e}_\theta \in L_2 \cap L_\infty$ and $\ddot{e}_\theta \in L_\infty$. Hence, Barbalat's lemma guarantees $\dot{e}_\theta \to 0$ as $t \to \infty$, which implies that the proposed composite adaptive position control system is globally stable. Figure 3 shows the complete diagram of the position control system.

5. EXPERIMENTAL RESULTS

The experimental equipment consists of a PC with 12-bit ADC and DAC interface card, a current-regulated voltage source inverter with two Hall-effect sensors for detecting stator phase currents, and a two-pole

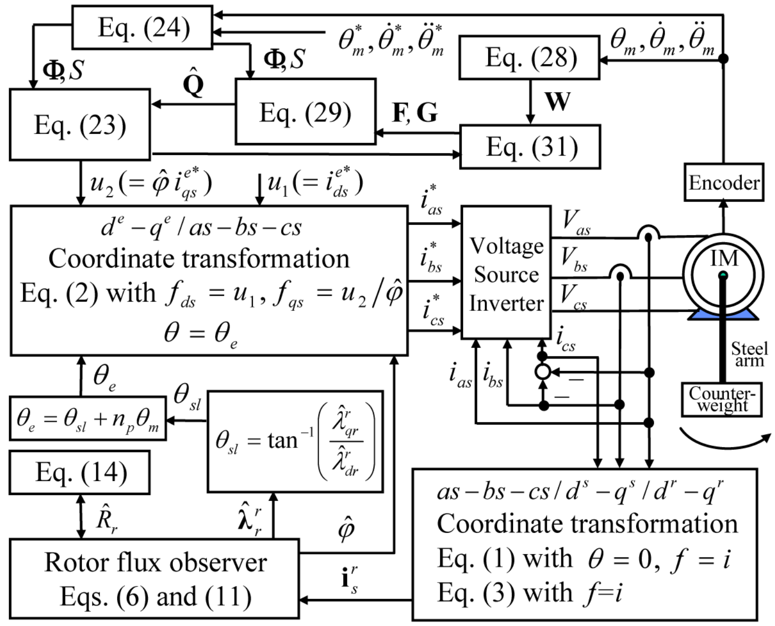

Fig. 3. Diagram of the composite adaptive position control system.

600-watt induction motor with a 1000 pulses/rev incremental encoder. The resolution of the encoder was improved by the four times frequency multiplier. A counterweight was affixed to the rotor shaft of the motor for simulating the variations of mechanical parameters and load torque disturbances. The diameter and mass of the counterweight were 5 cm and 500 grams, respectively. The length and mass of the steel arm were 16.4 cm and 246 grams, respectively. When the steel arm was approximately horizontal to the ground, the load torque was 1 Nm. The control algorithm was coded in C language and the sampling time was 0.2 ms. The following values of the parameters were used for the estimator and controller: $g_1 = 2.2,\ g_2 = 25,\ g_3 = 10,\ \kappa = 100,\ \delta = 0.98,\ u_1 = 2.3\,\mathrm{A_{rms}},\ \mathbf{\Lambda} = \mathrm{diag}[0.08\ \ 0.18\ \ 0.5]$, and $\mathbf{\Gamma}^{-1} = \mathrm{diag}[0.6\ \ 1.4\ \ 16]$.

In order to make a smooth-start (i.e., $\theta_m^*(0) = \dot{\theta}_m^*(0) = \ddot{\theta}_m^*(0) = 0$) and the signal vector $\mathbf{W}$ satisfy the persistent excitation condition, the position command was chosen as $\theta_m^* = \pi(1-e^{-10t})^2(\sin(t)+\sin(2t))$ rad. When a load torque $T_L = \sin(\theta_m)$ Nm was applied to the motor shaft, Fig. 4 shows the output responses for the nominal rotor resistance (R_r=1.14Ω) condition. As seen in Fig. 4b, the position tracking error varies from −0.9 to 1.8 degrees. The control algorithm needs 1.6 s to estimate the rotor resistance in Fig. 4c. From Fig. 4d, it is found that $\hat{J}_k$ fluctuates between 0.0114 and 0.0122. Based on the above condition, the constant k_t is 1.3845, therefore the percentage error of $\hat{J} = k_t\hat{J}_k$ is 4.9% in comparison with the formula in [16, p. 39]. As seen in Fig. 4f, $\hat{K}_k$ varies from 0.704 to 0.746. This means that $\hat{K}_L = k_t\hat{K}_k$ fluctuates between 0.975 and 1.033. Thus, the percentage error is 3.3% for the parameter $\hat{K}_L$ in estimating a load torque. Figure 5 shows the output responses for the 1.5 times nominal rotor resistance (R_r=1.71Ω). The designed estimator can estimate the rotor resistance well, as shown in Fig. 5b. However, the variations of rotor resistance affected the position response slightly. For all that, the estimated parameters, $\hat{J}_k$, $\hat{B}_k$, and $\hat{K}_k$ are all bounded. It is seen from Figs. 4 and 5 that the composite adaptive controller can estimate parameters well for the system because the position command contains two sinusoidal components. Hence, the estimated parameter vector $\hat{\mathbf{Q}}$ for the three mechanical parameters and the position tracking error converge to the actual values and zero, respectively. However, this sinusoidal signal with two distinct frequencies results in oscillatory behavior of the estimated parameters. In the above discussions, the proposed composite adaptive position controller has

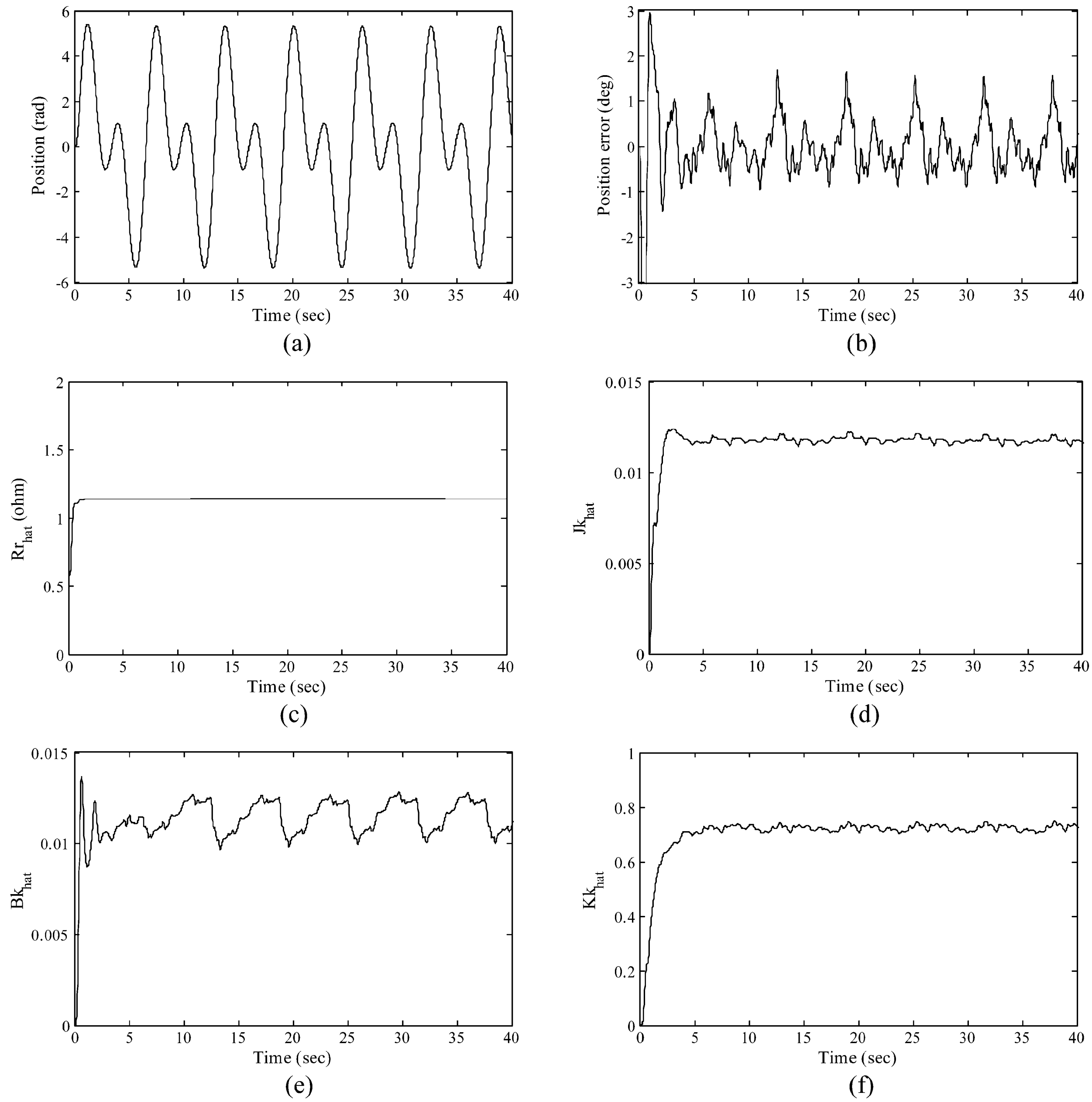

Fig. 4. Measured responses for the nominal rotor resistance condition: (a) position, θ_m (rad); (b) position error, e_θ (deg); (c) estimated rotor resistance, $\hat{R}_r$ (Ω); (d) estimated parameter, $\hat{J}_k$; (e) estimated parameter, $\hat{B}_k$; (f) estimated parameter, $\hat{K}_k$.

good position tracking capability, good load torque regulation, appropriate convergence for the estimated parameters, and robust with respect to the variations of mechanical parameters and the rotor resistance.

6. CONCLUSIONS

This paper has presented the rotor resistance estimation and the composite adaptive control for induction motor drives. The passive properties of the negative feedback connection from the rotor flux observer to

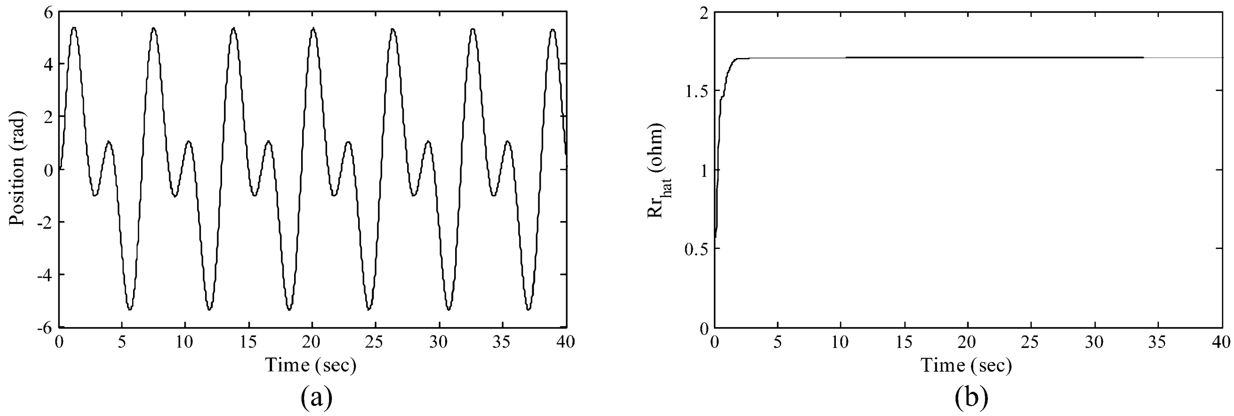

Fig. 5. Measured responses for 1.5 times of nominal rotor resistance condition: (a) position, θ_m (rad); (b) estimated rotor resistance, $\hat{R}_r$ (Ω).

the rotor resistance estimator, and the composite adaptive controller were proved. The control system was verified to be globally stable based on the passivity theorem, and robust with regard to the variations of motor mechanical parameters, rotor resistance, and load torque disturbances. It is shown that the proposed controller has good position tracking performance from the experimental results. In addition, the estimated parameters can converge to the actual values when the position command is sufficiently rich to satisfy the persistent excitation condition.

REFERENCES

1. Blaschke, F., “The principle of field orientation as applied to the new transvector closed-loop control system for rotating-field machines”, *Siemens Review*, Vol. 39, No. 5, pp. 217–220, 1972.
2. Bose, B.K., *Modern Power Electronics and AC Drives*, Prentice-Hall, 2002.
3. Willems, J.C., “Dissipative dynamical systems”, *Archive for Rational Mechanics and Analysis*, Vol. 45, No. 5, pp. 321–393, 1972.
4. Espinosa, G. and Ortega, R., “State observers are unnecessary for induction motor control”, *System and Control Letters*, Vol. 23, No. 5, pp. 315–323, 1994.
5. Gokdere, L.U. and Simaan, M.A., “A passivity-based method for induction motor control”, *IEEE Transactions on Industrial Electronics*, Vol. 44, No. 5, pp. 688–695, 1997.
6. Peresada, S., Tilli, A. and Tonielli, A., “New passivity-based speed-flux tracking controllers for induction motors”, In *Proceedings of the 26th Annual Conference of the IEEE Industrial Electronics*, Nagoya, Japan, pp. 1099–1104, October 22–28, 2000.
7. Petrovic, V., Ortega, R. and Stankovic, A.M., “Interconnection and damping assignment approach to control of PM synchronous motors”, *IEEE Transactions on Control System Technology*, Vol. 9, No. 6, pp. 811–820, 2001.
8. Travieso-Torres, J.C. and Duarte-Mermoud, M.A., “Two simple and novel SISO controllers for induction motors based on adaptive passivity”, *ISA Transactions*, Vol. 47, No. 1, pp. 60–79, 2008.
9. Achour, A.Y., Mendil, B. Bacha, S. and Munteanu, I., “Passivity-based current controller design for a permanent-magnet synchronous motor”, *ISA Transactions*, Vol. 48, No. 3, pp. 336–346, 2009.
10. Wei, M.-Y., Liu, T.-H. and Lin, C.-K., “Design and implementation of a passivity-based controller for sensorless synchronous reluctance motor drive systems”, *IET Electric Power Applications*, Vol. 5, No. 4, pp. 335–349, 2011.
11. Lenin, N.C. and Arumugam, R., “Vibration analysis and control in linear switched reluctance motor”, *Journal of Vibroengineering*, Vol. 13, No. 4, pp. 662–675, 2011.
12. Khalil, H.K., *Nonlinear Systems*. Prentice-Hall, 2002.
13. Narendra, K.S. and Annaswamy, A.M. *Stable Adaptive Systems*, Prentice-Hall, 1989.

14. Slotine, J.-J. E. and Li, W., *Applied Nonlinear Control*, Prentice-Hall, 1991.
15. Desoer, C.A. and Vidyasagar, M., *Feedback System: Input-Output Properties*, Academic Press, 1975.
16. Dawson, D.M. Hu, J. and Burg, T.C., *Nonlinear Control of Electric Machinery*, Marcel Dekker, 1998.